Junwei Su
Department of Mechanical Engineering,
University of Massachusetts Lowell,
One University Avenue,
Lowell, MA 01854
e-mail: junwei_su@student.uml.edu

Iman Mirzaee
Department of Mechanical Engineering,
University of Massachusetts Lowell,
One University Avenue,
Lowell, MA 01854
e-mail: iman_mirzaeekakhki@student.uml.edu

Fan Gao
Department of Chemical Engineering,
University of Massachusetts Lowell,
One University Avenue,
Lowell, MA 01854
e-mail: fan_gao@uml.edu

Xiao Liu
Department of Mechanical Engineering,
University of Massachusetts Lowell,
One University Avenue,
Lowell, MA 01854
e-mail: xiao_liu1@student.uml.edu

Majid Charmchi
Mem. ASME
Department of Mechanical Engineering,
University of Massachusetts Lowell,
One University Avenue,
Lowell, MA 01854
e-mail: majid_charmchi@uml.edu

Zhiyong Gu
Department of Chemical Engineering,
University of Massachusetts Lowell,
One University Avenue,
Lowell, MA 01854
e-mail: zhiyong_gu@uml.edu

Hongwei Sun[1]
Mem. ASME
Department of Mechanical Engineering,
University of Massachusetts Lowell,
One University Avenue,
Lowell, MA 01854
e-mail: hongwei_sun@uml.edu

Magnetically Assembling Nanoscale Metal Network Into Phase Change Material—Percolation Threshold Reduction in Paraffin Using Magnetically Assembly of Nanowires

A high throughput manufacturing process to magnetically assembling nanowire (NW) network into paraffin was developed for enhancing conductivity in phase change materials (PCMs) used in energy storage applications. The prefabricated nickel NWs were dispersed in melted paraffin followed by magnetic alignment under a strong magnetic field. Measuring electrical conductivity of the nanocomposite, as well as observing cross section of the sample slice under an optical microscope characterized the alignment of NWs. As a comparison, nickel particles (NPs) based paraffin nanocomposites were also fabricated, and its electrical conductivity with and without applied magnetic field were measured. The effects of aspect ratio of fillers (particles and NWs) and volume concentration on percolation threshold were studied both experimentally and theoretically. It was found that the NW based paraffin nanocomposite has much lower percolation threshold compared to that of particle based paraffin composite. Furthermore, the alignment of particles and NWs under magnetic field significantly reduces the threshold of percolation. This work provides solid foundation for the development of a manufacturing technology for high thermal conductivity PCMs for thermal energy storage applications.
[DOI: 10.1115/1.4029161]

Introduction

Ever-increasing energy demand, accelerated race to energy independency, and concern over environmental impact has significantly accelerated the development of renewable energy sources such as solar energy, geothermal energy, and wind energy. Most renewable energy sources of intermittent nature require effective energy storage systems. Latent heat storage is a particularly attractive technique due to its high capacity and its ability to store energy at near constant temperature corresponding to the phase transition temperature of PCM. The commonly used PCMs include paraffin waxes, fatty acids and their binary mixture, hydrate salt such as Glauder salt ($Na_2SO_4 \cdot H_2O$), and aromatics. However, the poor thermal performance has severely limited the application of current PCMs for high power, transient systems, and one of the major challenges facing energy industries such as renewable energies and waste heat recovery [1].

Great efforts, such as dispersing high conductive fillers in PCMs matrices [2,3] and dispersing PCMs in high conductive matrix [4], have been developed to improve the thermal conductivity of PCMs. PCM (paraffin) was filled in open-cell aluminum foams to form aluminum foam heat sinks by Hong and Herling in Ref. [5]. In another effort, micrometer (5 and 10 μm) long Ag and Cu NWs having a diameter of 25 nm fabricated using template

[1]Corresponding author.
Manuscript received August 26, 2014; final manuscript received September 15, 2014; published online December 10, 2014. Assoc. Editor: Hadi Ghasemi.

based method were mixed with polystyrene. The composites attained a low electrical percolation at 0.25 and 0.75 vol. % [6]. Similarly, the aspect ratio effect of Ag NWs on electrical percolation behavior was studied computationally and experimentally by White et al. [7]. Ni NW filled with P(VDFTrFE) copolymer nanocomposites were prepared with a volume fraction varying from 0 to 5 vol. %, and an electrical percolation threshold at 0.75 vol. % was achieved. In addition, an electrical conductivity of 10^2 S m^{-1} was observed for the composites at 5 vol. % using NWs with aspect ratio ~250 [8]. Abramson et al. achieved significant improvement in thermal conductivity of parylene by growing boron-doped Si NW array as matrix in parylene [9]. The order of magnitude improvement was reported with a low filling factor (2%). However, due to the expensive and complex equipment for fabrication, the NW array filled PCMs are hardly to be applied in large scale industry.

The aim of this work is to explore a high throughput manufacturing process to synthesize and embed metallic NW network into nanoPCMs using magnetic field driven assembly of NWs. At the end of this process, dispersed columns of well aligned NWs are formed in PCMs. Electrical conductivity of this nanoPCM was compared with the prediction of percolation theory. Experimental study shows the magnetically aligned PCMs composites can achieve a much lower percolation threshold than the randomly dispersed PCMs composites.

Experimental Methods

The nickel (Ni) NWs were synthesized using well-known template based fabrication method. First, a thin layer of Ag was thermally evaporated on one face of a commercially available anodized alumina (AAO) membrane (GE Healthcare) and formed a conductive layer. The AAO membrane with the Ag contact was placed on a smooth copper plate and restrained by a glass joint and an O-ring seal. The membrane was soaked in de-ionized (DI) water for 5 min and then filled with the Ni electrolyte (Nickel Sulfamate Bath RTU, from Techni Inc.) for electroplating process. The plating current was set at 2 mA/cm^2 for the Ni NW growth. The length of NWs was controlled by the duration of the applied current. After Ni NW growth, the Ag layer on the AAO membrane was dissolved in the etching solution (the mixture of methanol, 35 wt.% hydrogen peroxide and ammonium hydroxide with the ratio of 4:1:1). Last, after being rinsed several times in water, the membrane was dissolved in 2 M NaOH to release the Ni NWs. The released Ni NWs were rinsed by water and finally stored in the ethanol. Figure 1 presents the schematic of NWs synthesis method, and Fig. 2 shows the scanning electron microscope (SEM) pictures of NPs and fabricated NWs. The Ni NWs have a length of 5–8 μm and a diameter of 200 nm. The SEM image confirms the dimension and smooth surface of nickel NWs.

The preparation for particle and NW based paraffin composites follows the same procedure as illustrated in Fig. 3. NPs (diameter-$< 5\,\mu$m), purchased from Sigma Aldrich has resistivity around 6.97 $\mu\Omega$ cm at 20 °C. Paraffin wax, also purchased from Sigma Aldrich, has a density of 900 kg/m^3 and the melting point of 55 °C, which was determined by differential scanning calorimeter measurement. The electrical conductivity of the paraffin is around 10^{-13} S m^{-1} at room temperature. The paraffin wax was heated up to 120 °C first. The ethanol solution containing NPs was slowly added into melted paraffin wax and ethanol in the paraffin was evaporated in about 10 min. Then the mixture was uniformly dispersed in an ultrasonicator (55 W) for 2 min at 80 °C. As a result, a suitable dispersion of NWs and particles in paraffin wax was achieved. For nanoPCMs that did not require magnetic alignment, the paraffin composites samples were immersed in cold water for a rapid solidification in order to avoid the sedimentation of fillers. Otherwise, the sample was placed in a 0.5 T magnetic field for 10 s, and then was solidified in water for 20 s with magnetic field on (Fig. 3).

After nanoPCMs preparation procedure was completed, the sample was cut into slices in the direction parallel to the magnetic direction for morphology inspection. Optical microscope

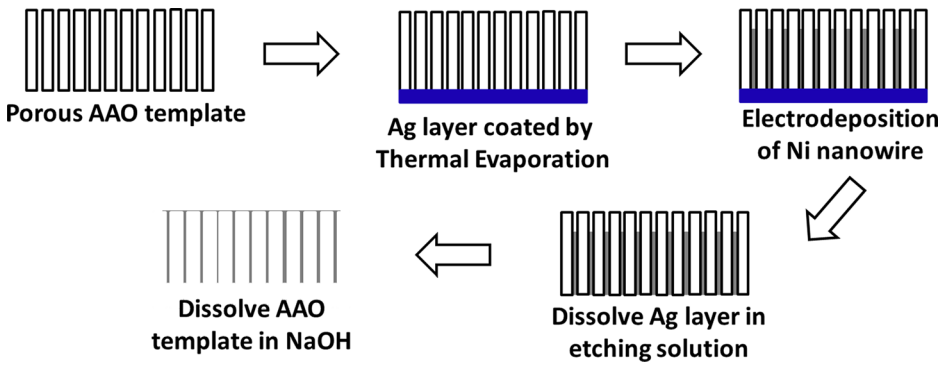

Fig. 1 Schematic of NW synthesis process

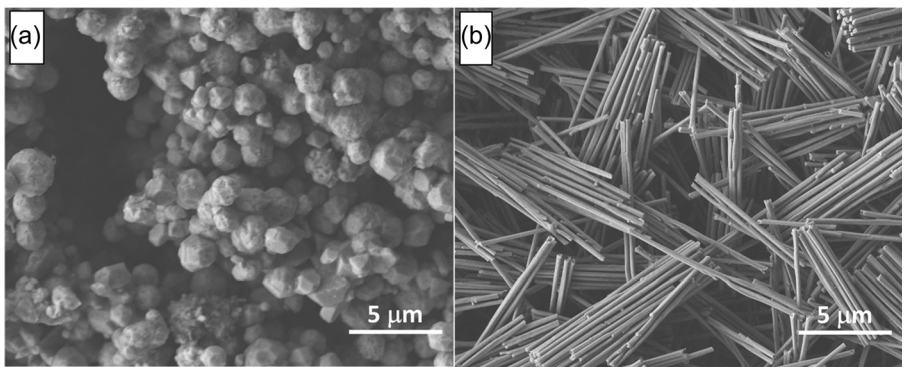

Fig. 2 SEM images of (*a*) NPs and (*b*) nickel NWs

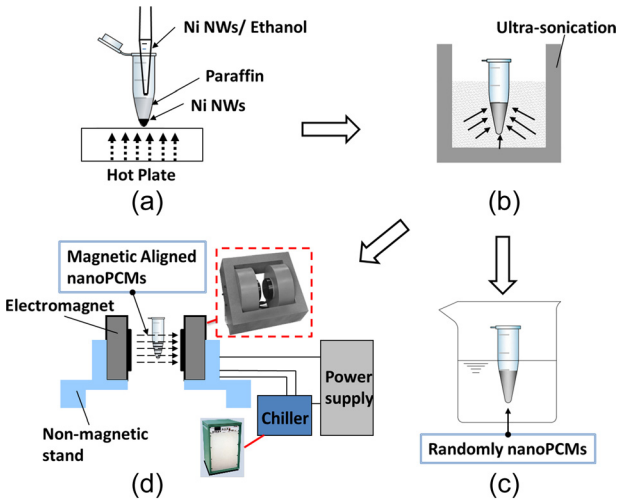

Fig. 3 Schematic of nanoPCMs preparation process: (*a*) adding the NWs suspension into melted paraffin. (*b*) Ultrasonication of the mixture at 80 °C to obtain a uniform distribution of fillers. (*c*) Rapid solidification in water for randomly distributed NWs in PCMs. (*d*) Applying magnetic field to obtain align NWs in PCMs.

(ACCU-Scope 3032) was used to observe the cross section of sliced nanoPCM sample as shown in Fig. 4. It is apparent that the magnetic field helps significantly improve the NW alignment in the magnetic field direction.

After the preparation of nanoPCMs, the samples were subjected to two-probe I–V measurement under ambient condition, using high resistance electrometer (Keithley 6517B). During the measurement, two-probe tips (Signatone) having a distance of 1 mm from each other were punched a millimeter into the PCM composites samples to eliminate the contact resistance effects. For the magnetically aligned samples, i.e., NWs and particles, the probe tips were placed in the direction of magnetic aligned columns. As a comparison, the electrical conductivity in the direction perpendicular to the aligned columns was also obtained. In all cases, the measurements were conducted by sourcing voltage and measuring current.

Theory of Percolation Threshold

According to percolation theory, electrical conductivity of composite is highly dependent on volume fraction p and aspect ratio (length to radius) of the fillers [10]. The conductivity is described by a power law equation given by

$$\sigma = \sigma_o(p - p_c)^t \tag{1}$$

where σ_o is a constant and t is the critical exponent. p_c is the percolation threshold. The percolation threshold model is based on excluded volume model [11,12]. The excluded volume for capped cylinders is given by [13]

$$V_{ex,nw} = (32\pi/3)R^3 + 8\pi LR^2 + 4L^2R\sin\gamma \tag{2}$$

where L is the length of the NWs and R is its radius. The γ is the angle between two NWs. For randomly oriented NWs, $\sin\gamma$ is equal to $\pi/4$. Therefore, if NWs were dispersed randomly in the composite, the Eq. (2) becomes

$$V_{ex,nw} = (32\pi/3)R^3 + 8\pi LR^2 + \pi L^2R \tag{3}$$

While for spherical particles, the excluded volume is calculated as

$$V_{ex,np} = (32\pi/3)R^3 \tag{4}$$

The excluded volume of fillers is related to the critical number of nanofillers (N_c) required for percolation by

$$N_c \approx \frac{V}{V_{ex}} \tag{5}$$

where V is the total sample volume. With the uniform distribution assumption, the percolation thresholds for aligned and randomly dispersed NWs can be calculated as

$$p_{c,nw} = \frac{N_c(4\pi R^3/3 + \pi R^2 L)}{V} = \frac{V(4\pi R^3/3 + \pi R^2 L)}{V \times V_{ex,nw}} = \frac{(4\pi R^3/3 + \pi R^2 L)}{(32\pi/3)R^3 + 8\pi LR^2 + \pi L^2 R} \tag{6}$$

However, for particle filled sample, the percolation threshold is a constant 12.5%.

Results and Discussion

Samples of nanoPCMs composites were prepared with a volume fraction of Ni NWs varying from 0 to 15 vol. % and Ni particles varying from 0 to 50 vol. %. The DC electrical conductivities of the Ni particles and NWs paraffin samples are plotted as a function of the particle volume fraction in Fig. 5(*a*). As can be seen, the electrical conductivity increases significantly, by several orders of magnitude, at 5 vol. % for the Ni NW PCM compared to 15 vol. % observed for Ni particles. The particle data is fitted based on Eq. (1) with $p_c = 12.5$ vol. %, $t = 3.58 \pm 0.73$, and $\sigma_o = 1.43 \times 10\,\mathrm{S\,m^{-1}}$. σ_o is an extrapolation at 100 vol. % of Ni particles, which corresponds to the conductivity of NPs. From our results, σ_o is two orders of magnitude lower than the conductivity reported by Sigma Aldrich. The NW data is best-fitted by a scaling law according to Eq. (1) with $p_c = 2$ vol. %, $\sigma_o = 4.98 \times 10^4\,\mathrm{S\,m^{-1}}$, and $t = 4.98 \pm 0.51$. σ_o is the same order of magnitude the conductivity previously measured in Ni NWs [14].

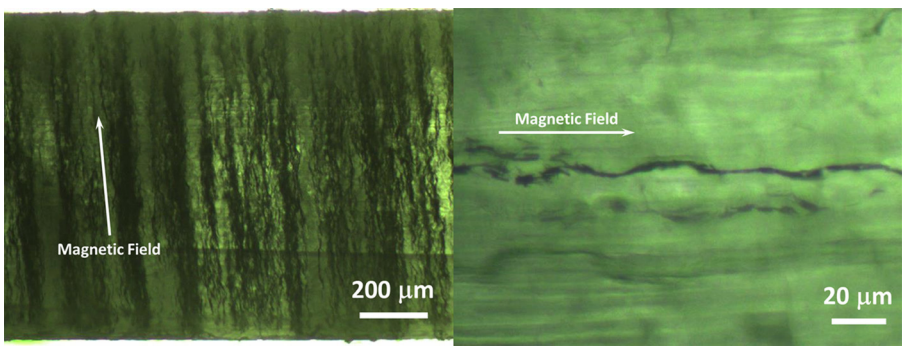

Fig. 4 Optical microscopic images of magnetic aligned NWs PCM sample with 0.1 vol. % volume ratio (magnetic direction is shown by arrows)

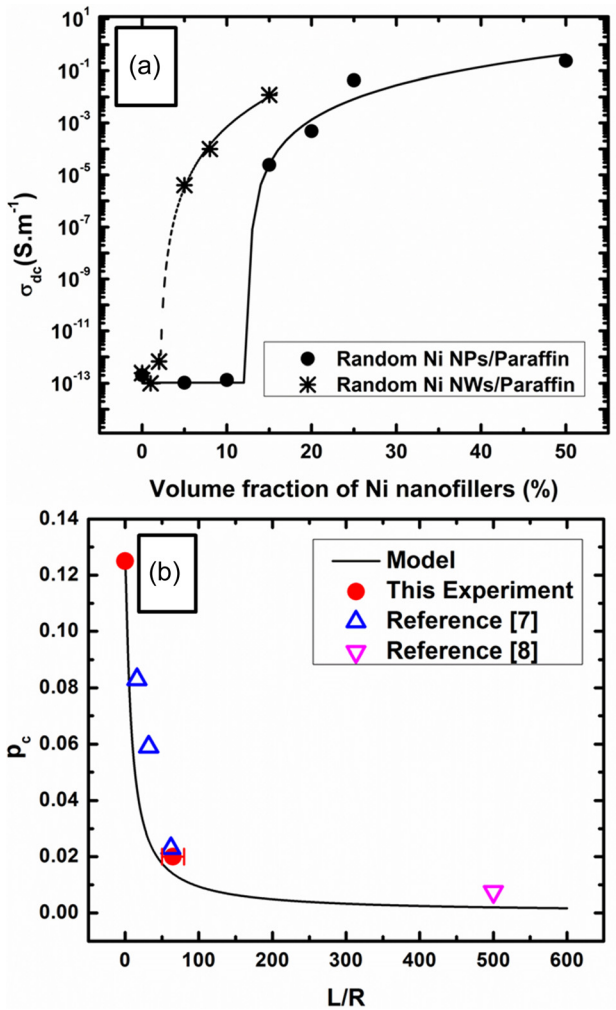

Fig. 5 (*a*) Dependence of the DC conductivity (σ_{dc}) on the nickel nanofiller volume fraction in paraffin matrix at 25 °C. (*b*) p_c versus *L/R* from experiments and the excluded volume analytical model.

Figure 5(*b*) shows the dependence of percolation threshold on aspect ratio of nanofillers according to excluded volume model. For Ni particles, the experimental value of percolation threshold is similar to the theoretical value, which is 12.5 vol. %. For Ni NWs, we find a critical volume fraction of 1.46 ± 0.31 vol. % according to Eq. (6), which is slightly lower than the experimental value of 2 vol. %. This difference can be explained by the formation of some poorly dispersed NW bundles, since the excluded volume model is highly dependent on the ability to disperse individually and uniformly the NWs in the matrix [10].

Figure 6 presents the comparison of electrical conductivity of random NPs in paraffin with magnetically aligned NPs in the paraffin. The percolation threshold value (p_c) for magnetically aligned NPs paraffin is much lower than that of randomly dispersed NPs paraffin due to formation of anisotropic nickel network in PCMs at lower filler volume fraction. The NPs paraffin percolation threshold is reduced to 4.5 vol. % after assembling with 0.5 T magnetic fields. Even in high volume fraction zone (>12.5 vol. %), the 0.5 T magnetic field also enhances the electrical conductivity by two orders of magnitude at the same volume fraction. The percolation threshold decrease has significant meaning for energy storage system. The lower percolation threshold would make PCMs obtain higher conductivity with less filler ratio. In the other words, the magnetic aligned PCM composites would store more energy at constant temperature with high thermal conductivity.

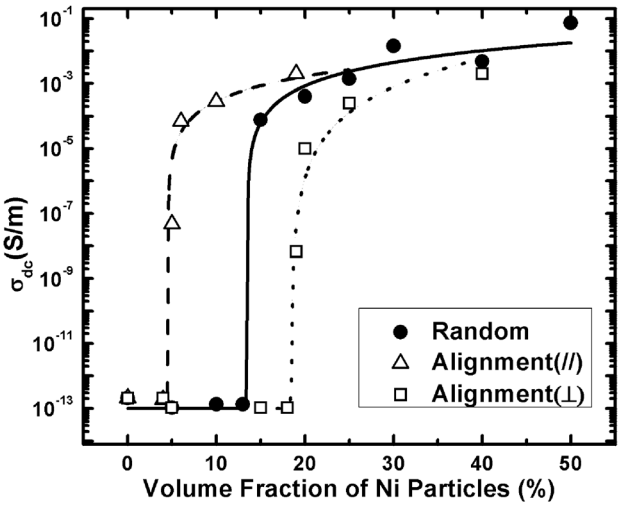

Fig. 6 Dependence of the DC conductivity (σ_{dc}) on the NPs volume fraction in paraffin matrix at 25 °C for random Ni NPs/paraffin system (•), and for magnetic aligned Ni NPs/paraffin system in parallel direction (◁), and in perpendicular direction (□). The lines correspond to the best linear fitting.

The slope of the best fitting line (t) increases from 3.58 ± 0.73 to 6.03 ± 0.48 by applying magnetic field, and the aligned value exceeds the theoretically predicted one ($t \approx 2.0$). This effect can be explained by nonstatistical order distribution of conductive phase in PCM matrix, since value $t \approx 2$ is provided by random (statistical) distribution of conductive particles in nonconductive PCMs [10].

Figure 7 reports the comparison between randomly distributed Ni NWs in paraffin and magnetically aligned Ni NWs in the paraffin. A similar effect of the magnetic field on percolation threshold can also be observed. The percolation threshold of Ni NW paraffin system could be reduced from 2 vol. % to 1 vol. % by 0.5 T magnetic fields assembling.

The magnetic aligned NWs based PCM composites could acquire even lower percolation threshold than particles based PCM composites. So the magnetic aligned NW based PCM

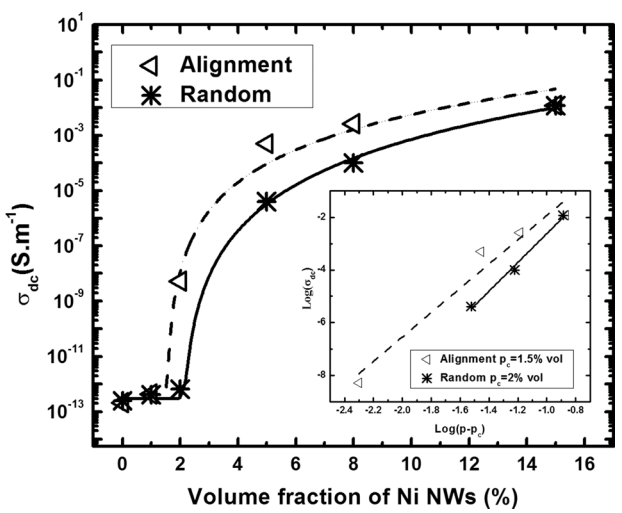

Fig. 7 Dependence of the DC conductivity (σ_{dc}) on the nickel NWs volume fraction in paraffin matrix at 25 °C for random Ni NWs/paraffin system (✱), and for magnetic aligned Ni NWs/paraffin system (◁). The inset shows the log–log plot of σ_{dc} versus $(p - p_c)$. For the random Ni NWs/paraffin, $p_c = 2\%$. For the magnetic aligned Ni NWs/paraffin, $p_c = 1\%$. The lines correspond to the best linear fitting.

composites would have better performance when it was applied as energy storage materials.

Conclusion

A high throughput manufacturing process to magnetically assembling NW network into paraffin was developed for enhancing conductivity in energy storage materials. The comparisons of electrical percolation thresholds, p_c, for networks of particles with that of NWs were performed and analytical model was used to explain the experimental observation successfully. Low percolation thresholds were found in magnetically aligned NPs and NWs nanocomposites systems. By using high aspect ratio Ni NWs as nanofiller, the percolation threshold could be reduced to a much lower level than Ni particles.

Acknowledgment

The authors are grateful for the support from Tektronix Inc. for providing Keithley 6517B electrometer and the National Science Foundation (CMMI 1348098) for funding this research.

References

[1] Stritih, U., 2003, "Heat Transfer Enhancement in Latent Heat Thermal Storage System for Buildings," Energy Build., **35**(11), pp. 1097–1104.
[2] Frusteri, F., Leonardi, V., Vasta, S., and Restuccia, G., 2005, "Thermal Conductivity Measurement of a PCM Based Storage System Containing Carbon Fibers," Appl. Therm. Eng., **25**(11–12), pp. 1623–1633.
[3] Zeng, J. L., Cao, Z., Yang, D. W., Sun, L. X., and Zhang, L., 2010, "Thermal Conductivity Enhancement of Ag Nanowires on an Organic Phase Change Material," J. Therm. Anal. Calorim., **101**(1), pp. 385–389.
[4] Py, X., Olives, R., and Mauran, S., 2001, "Paraffin/Porous-Graphite-Matrix Composite as a High and Constant Power Thermal Storage Material," Int. J. Heat Mass Transfer, **44**(14), pp. 2727–2737.
[5] Hong, S. T., and Herling, D. R., 2006, "Open-Cell Aluminum Foams Filled With Phase Change Materials as Compact Heat Sink," Scr. Mater., **55**(10), pp. 887–890.
[6] Gelves, G. A., Lin, B., Sundararaj, U., and Haber, J. A., 2006, "Low Electrical Percolation Threshold of Silver and Copper Nanowires in Polystyrene Composites," Adv. Funct. Mater., **16**(18), pp. 2423–2430.
[7] White, S. I., Mutiso, R. M., Vora, P. M., Jahnke, D., Hsu, S., Kikkawa, J. M., Li, J., Fischer, J. E., and Winey, K. I., 2010, "Electrical Percolation Behavior in Silver Nanowire Polystyrene Composites: Simulation and Experiment," Adv. Funct. Mater., **20**(16), pp. 2709–2716.
[8] Lonjon, A., Laffont, L., Demont, P., Dantras, E., and Lacabanne, C., 2009, "New Highly Conductive Nickel Nanowire-Filled P(VDF-TrFE) Copolymer Nanocomposites: Elaboration and Structural Study," J. Phys. Chem. C, **113**(28), pp. 12002–12006.
[9] Abramson, A. R., Kim, W. C., Huxtable, S. T., Yan, H., Wu, Y., Majumdar, A., Tien, C. L., and Yang, P., 2004, "Fabrication and Characterization of a Nanowire/Polymer-Based Nanocomposite for a Prototype Thermoelectric Device," J. Microelectromech. Syst., **13**(3), pp. 505–513.
[10] Stauffer, D., and Aharony, A., 1991, *Introduction to Percolation Theory*, Taylor and Francis, London, UK.
[11] Bug, A. L. R., Safran, S. A., and Webman, I., 1985, "Continuum Percolation of Rods," Phys. Rev. Lett., **54**(13), pp. 1412–1415.
[12] Bug, A. L. R., Safran, S. A., and Webman, I., 1986, "Continuum Percolation of Permeable Object," Phys. Rev. B, **33**(7), pp. 4716–4724.
[13] Balberg, I., and Binenbaum, N., 1984, "Percolation Thresholds in the Three-Dimensional Sticks System," Phys. Rev. Lett., **52**(17), pp. 1465–1468.
[14] Ou, M. N., Yang, T. J., Harutyunyan, S. R., Chen, Y. Y., Chen, C. D., and Lai, S. J., 2008, "Electrical and Thermal Transport in Single Nickel Nanowire," Appl. Phys. Lett., **92**(6), p. 063101.